

# INFLUENCE OF LIGHTNING STRIKES ON PHOTOVOLTAIC MODULES PROPERTIES

I.Naxakis, V. Perraki and E. Pyrgioti  
Department of Electrical and Computer Engineering, University of Patras, GREECE  
Patras-Rio, Greece 26500  
mail to: [naxakis@ece.upatras.gr](mailto:naxakis@ece.upatras.gr)

**ABSTRACT:** The objective of this work is to present how modules react in case of lightning strikes and overvoltages. The experimental process included the application of impulse voltages within the limits specified by the standards as well as, beyond these limits. After each impulse voltage stress, the properties of the stressed photovoltaic module were compared with those of one with identical characteristics unstressed module in order to evaluate possible modifications in the stressed module properties. The measurements were gathered with the use of a PVPM power measuring device. The conclusions were extracted after completion of an extensive series of tests. The results confirmed that, after the completion of the tests, the tested module had not undergone power degradation, had not shown any evidence of surface defects and continued to operate reliably.

**Keywords:** photovoltaic, module properties, Impulse voltage, regulations

## 1 INTRODUCTION

The widespread adoption of the photovoltaics (PVs) forming grid connected or standalone electrical applications is a dominant issue nowadays. The ecological destruction caused by the excessive use of polluting fuels in order to increase the electricity production and the exhaustion of conventional energy deposits has pushed towards this direction. However, while photovoltaic are the fastest growing power generation technology worldwide, their growth raises new questions. For example, a difficult issue is whether the usual lightning protection system of a PV installation is sufficient under the burden of current rapid developments. In general, photovoltaic facilities are more vulnerable to direct lightning strikes than conventional low voltage (LV) power distribution systems due to their inherently uncovered locations on roofs and facades of buildings and on wide unsheltered areas. Installation of earth electrodes and ground wires has been not only the primary method for the protection of the electrical systems, (such as a photovoltaic system) but also a developing technology [1], [2], [3]. The reliable protection of valuable photovoltaic installations and their electronics against overvoltages and current surges are of great importance. [4-6]. It should be mentioned that the field experience is limited and the applied protective systems do not follow a general rule. In relevant literature there is not enough information available about the PV module behavior against lightning strikes and overvoltages. In this paper the standard IEC 61730-2 [7] was used which refers to photovoltaic module safety qualifications. The IEC 61730-2 outlines in detail many electrical and mechanical tests that have been designed to ensure efficient operation and safety over time, concerning the properties and materials of photovoltaic modules. The impulse voltage test, which is a part of [7] simulates an atmospheric event such as a lightning strike and is one of the last tests that must be conducted. Extended tests have been conducted at the Electrical and Computer Engineering Department at the University of Patras in Greece, presenting research which is related to the effect of temperature [8] as well as to the effect of solar irradiation [9] on the properties of the PV modules. Moreover, with this work the response of a photovoltaic module against a potential standard lightning strike has been experimentally studied using a high impulse voltage generator (up to 400 kV).

## 2 IMPULSE VOLTAGE TEST

One of the final tests, included in IEC 61730-2, is the impulse voltage test which must be conducted with acceptable results. This test is performed only for modules classified as application classes A and B, and differs in terms of requirements for each class [7]. Modules which are classified as Class A are stressed with higher impulse voltages than modules which are classified as Class B. The impulse voltage is based on the maximum system voltage of the module. For example, if the maximum system voltage is 1000 V, application Class A modules have to be tested with 8 kV (impulse voltage peak) while application Class B modules with 6 kV. Table I shows the Impulse voltage in relation to the maximum system voltage, in accordance with IEC 61730-2.

**Table I:** Impulse voltage versus maximum system voltage according to IEC 61730-2

Maximum System Voltage	Impulse Voltage - Application Class A	Impulse Voltage - Application Class B
1000 V	8000 V	6000 V

The tests were always conducted at room temperature conditions (19.5 °C - 21 °C, 745 mmHg - 755 mmHg) and relative humidity of less than 75%. The impulse voltage generator was set to deliver a 1.2/50  $\mu$ s Impulse Voltage waveform (Figure 1) according to [7]. During the test, there was no evidence of dielectric breakdown or surface tracking of the module, so the test was considered successful [7].

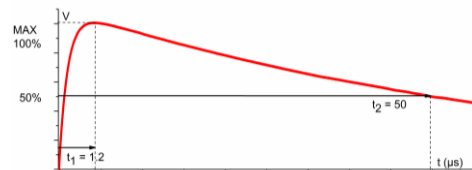


**Figure 1:** Impulse voltage waveform 1.2 / 50  $\mu$ s. 1.2  $\mu$ s is the front time and 50  $\mu$ s is the time to half-value

The impulse voltage waveform was applied by the impulse voltage generator shown in Figure 2 while the front time and duration was constantly checked by an oscilloscope (Tektronix DPO 4014) which follows the IEC

### 3 EXPERIMENTAL PROSEDURE

This work studies the effect of lightning on the performance of the PV modules. Different values of impulse voltages were applied on two photovoltaic modules, with the specifications shown in Table II, (Luxor LX-200M - made of monocrystalline silicon cells). The properties of a stressed module (module B) were compared with those of an unstressed reference module (module A) of the same specifications.

**Table II:** The specifications of the tested modules at STC provided from manufacturer

Electrical Data	LX-200M
$P_{max,STC}$ [Wp]	200
$P_{max,STC}$ Range	201.50-206.49
$I_{max}$ [A]	5.39
$V_{max}$ [V]	37.39
$I_{sc}$ [A]	5.87
$V_{oc}$ [V]	44.27
Maximum systems voltage	1000 V



**Figure 2:** View of the impulse-voltage generator



**Figure 3:** Photovoltaic outdoor measuring set up

The characteristic curves were plotted with the use of the PVPM 2540C, which plots the current-voltage (I-V) and the power-voltage (P-V) curves of the photovoltaic modules. Through, a patented procedure the device calculates the module's most important parameters, such as open circuit voltage ( $V_{OC}$ ), short circuit current ( $I_{SC}$ ), voltage and current at the maximum power point ( $V_{pmax}$  and  $I_{pmax}$ ), peak power ( $P_{max}$ ), maximum power at standard test conditions ( $P_{max,STC}$ ), fill factor (FF), series resistance ( $R_s$ ) and parallel resistance ( $R_p$ ). The collected data were transferred into a computer and were evaluated. The experimental devices for the impulse voltage tests were installed in the High Voltage Laboratory (Figure 2), whereas the devices for the evaluation of the PV properties (Figure 3) were installed on the roof at the building of the Electrical and Computer Engineering Department, at the University of Patras in Greece. In the preparatory phase, I-V and P-V characteristic curves were plotted in order to see whether the modules are identical and whether their properties comply properly with the manufacturer's specifications. Then extensive outdoor measurements were carried out and I-V and P-V curves of the tested modules were plotted corresponding to a variety of different irradiances and temperatures. Important

electrical characteristics were observed. At this point it is of great importance to mention that the measurements, gathered in order to choose the appropriate ones for the comparison between the modules, lasted more than three years while the experiments on the PV modules are still under development. The results selected were the ones obtained during periods of day, with as much stable sunshine as possible and around solar noon. In that case, all the sets of measurements were conducted simultaneously for both modules, with the same PVPM and the same sensors. Therefore, the comparison of the module's photovoltaic properties was made between the plots delivered from both modules performed under almost equal irradiances and temperatures. The impulse voltage generator that was used in the next steps had to be adjusted to deliver the appropriate Impulse Voltage amplitude. "Module B" was stressed with impulse voltages into the limits of the standards as well as with voltages beyond the limits [10]. After each voltage stress, measurements were gathered and I-V and P-V curves were created in order to compare them with the ones from the unstressed "module A". At the same time, the maximum power,  $P_{max}$ , was recorded in order to evaluate possible modifications in the module B properties.

### 4 RESULTS

The results presented in this work, refer to commercially available monocrystalline silicon modules. The I-V and P-V characteristics extracted from measurements conducted under outdoor conditions focus on the influence of different values of impulse voltages (simulating lightning and surge conditions) on the photovoltaic parameters of the selected modules.

Figure 4(a) presents the I-V and P-V characteristics which were plotted for modules A and B in the preparatory phase. The comparison based on the formulation of these characteristics as well as on the maximum power of both modules shows a slight non-significant difference for voltages equal or higher than the  $V_{max}$  as to the current and power. These pre measures, indicating that the two modules are not entirely similar, may, nevertheless, justify future divergences between their results.

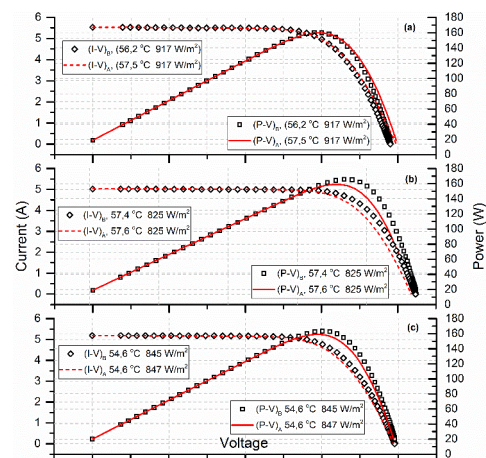


**Figure 4:** P-V and I-V curves. (a) Before stress. (b) After stress with 6 kV. (c) After stress with 8 kV

The I-V and P-V curves extracted from module A and the stressed module B with the impulse voltage 6 kV are shown in Figure 4(b) (Application Class B). The

maximum power generated from this module was slightly higher (for a little lower temperature) than from the unstressed module, while the values of  $V_{OC}$  and  $I_{SC}$  remained almost the same.

In Figure 4(c), module B has been stressed with an impulse voltage of 8 kV (within the limits of the regulation specifications - Application class A). A non-significant difference in the values of maximum power (less than the observed in Figure 4(b)) is observed, for slightly different irradiation, while the same values of  $V_{OC}$  and  $I_{SC}$  are recorded for the two modules. Even though the regulations require the realization of tests with impulse voltage 6 kV and 8 kV, the amplitude of the developing overvoltage in a real installation can be significantly greater, exceeding the value of 30 kV [11]. This statement has been confirmed by simulation studies in our laboratory with the help of the Alternative Transients Program - Electromagnetic Transients Program (ATP - EMT) [12]. For the above reasons, the experimental process was chosen to continue with test voltages beyond the limits set by the standards.

In Figure 5 the unstressed and stressed module I-V and P-V curves are compared for the cases where module B is stressed with 10 kV, 20 kV and 25 kV impulse voltages. Even though, the used impulse voltage far exceeded the limits dictated by the standards, the I-V and P-V curves of the two modules have the same form as in the previous cases. However, as seen in Figure 5(b), the maximum power delivered from module B (stressed with 20 kV impulse voltage) is a little higher than the power from module A, while the values of  $V_{OC}$  and  $I_{SC}$  remain almost the same. This result could be attributed to the slight difference in temperature between them. No differences are shown in the performances between the two modules in Figure 5(a) and Figure 5(c).

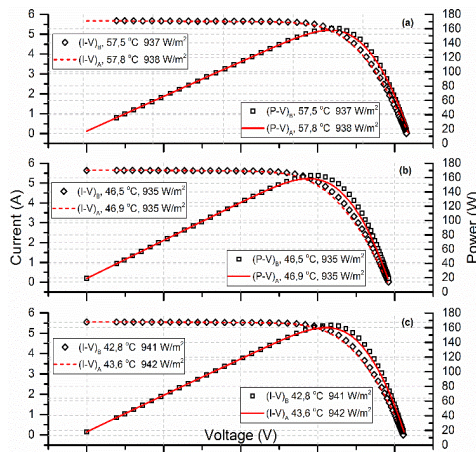


**Figure 5:** P-V and I-V curves. (a) After stress with 10 kV. (b) After stress with 20 kV. (c) After stress with 25 kV

As no substantial differences between the plots corresponding to module A and B (stressed up to 25 kV) are observed, it was decided to test the module with impulse voltages up to 35 kV. The P-V curves of module B after stressed with 32 kV and 35 kV impulse voltages, respectively, (Figure 6(a) and Figure 6(c)) are almost identical with those of module A. The graphs which correspond to the stress with 34 kV impulse voltage (Figure 6(b)) show that module B has a slightly higher peak power than module A, while the values of  $V_{OC}$  and  $I_{SC}$  are almost the same.

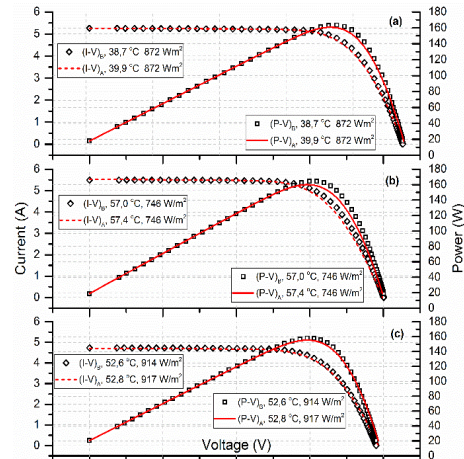


**Figure 6:** P-V and I-V curves. (a) After stress with 32 kV. (b) After stress with 34 kV. (c) After stress with 35 kV

During the application of the impulse voltages, in the last set of tests, however, the voltage waveform presented some interesting changes shown in Figure 7. Figure 7 depicts the waveform of the stress test with 32 kV impulse voltage. The result of the activation of the impulse voltage generator with open circuit configuration is indicated with the outer (red) line. The inner (black) line depicts the waveform after the module was connected to the impulse voltage generator.

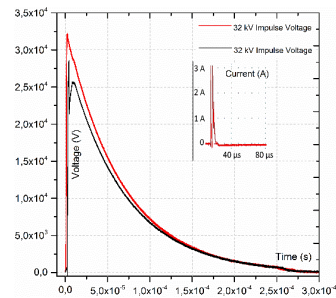


**Figure 7:** Stress impulse voltage and leakage currents

The maximum voltage in this case was reduced to 28 kV and the waveform differed from the typical. The instantaneous voltage drop and the very fast comeback of the voltage to the typical impulse voltage waveform (1.2/50  $\mu s$ ) indicates air breakdown at the surface of the protective glass of the module and rapid recovery afterwards. At the same time, surface creep currents of 3 A maximum value were recorded at the peak of the voltage. The current ripple lasted only 10  $\mu s$  and the energy released (0.29 mWh) due to the air breakdown was not significant. Small surface discharges (3 - 4 mm) were visible during this test. Testing with impulse voltage higher than 32 kV shown that the electrical discharges on the air above the module's surface are multiplied. After this stress test, the module, once again, seemed to perform without any significant change in its properties.

Moreover, Figure 8 presents the effect of the application of the impulse voltage to module B onto the module's output power (Figure 8(a)) as well as the effect of irradiance onto the modules output power (Figure 8(b)). More specifically, Figure 8(a) illustrates the ratio of the measured maximum output power to the maximum output power indicated by the manufacturer for module B ( $P_{B,max}/P_{man}$ ), as a function of the test impulse voltage

(blank squares symbols). In the same figure the ratio of the maximum output power calculated under standard test conditions is also presented, (delivered by the PMPM measuring device), to the maximum output power indicated by the manufacturer, ( $P_{B,STC}/P_{man}$ ), as a function of the test impulse voltage (blank circular symbol). A negligible slope is observed, through the linear fit of  $P_{B,max}/P_{man}$  and  $P_{B,STC}/P_{man}$  as a function of the test impulse voltage, which cannot, however, confirm permanent degradation of the module's B power. Figure 9(b) shows the ratio of the measured maximum output power to the maximum output power at STC for module B, ( $P_{B,max}/P_{B,STC}$ ) as a function of the corresponding irradiance (blank square symbols) and for module A ( $P_{A,max}/P_{A,STC}$ ) as a function of the corresponding irradiance (x cross symbols). From the linear fitting on the  $P_{B,max}/P_{B,STC}$  and  $P_{A,max}/P_{A,STC}$ , we confirm that the reduced performances of the two modules A and B are always the same. The only difference between the linear fittings is a negligible variation in irradiances above 1000  $W/m^2$ , which however is not enough to change the overall conclusion. Therefore, module B which has suffered multiple stresses by applying impulse voltages has not sustained degradation of its properties.

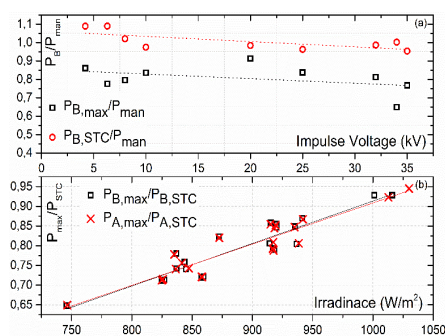


**Figure 8:** P-V and I-V curves. (a)  $P_{B,max}/P_{man}$  and  $P_{B,STC}/P_{man}$  versus impulse voltage. (b)  $P_{B,max}/P_{B,STC}$  and  $P_{A,max}/P_{A,STC}$  versus irradiance.

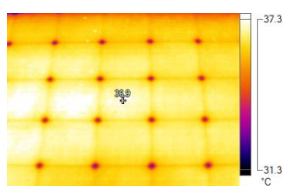


**Figure 9:** representative IR image for both modules

In parallel to the basic tests with the impulse voltages application on the modules a series of visual observations (Figure 9) and measurements were conducted with an infrared (IR) camera (Fluke Ti32 Thermal Imager). Thermal images of module A and B were initially taken (before the impulse voltage stress test) by using the IR camera. The thermal images captured for both the modules in every step of the procedure shown no evidence of damage. Figure 10 shows the characteristically form of the thermal image for both the modules which remained unchanged after every implementation of the voltage.

## 6 CONCLUSIONS

To sum up, in this work impulse voltages into the limits specified by the standards (6 kV, 8 kV), as well as beyond these limits (20 kV, 32 kV, 34 kV and 35 kV) were applied on a photovoltaic module in order to assimilate

lightning and surge stress conditions on photovoltaic installations. The performance of module A with the properties of a similar unstressed module B (through the I-V, the P-V curves and the  $P_{max}$  values) was initially compared and it was noticed that the module successfully passed the tests showing that its performance was not degraded and it could reliably operate. Subsequently, we compared the properties of both modules for many different values of solar irradiation which correspond to different temperatures.

Comparison of a series of visual observations which were realized with an infrared (IR) camera has shown a smooth operation of the module both before and after the stress tests. Differences of the thermal behaviour in each photovoltaic cell were not observed either. Therefore, although module B has suffered multiple stresses, no induced degradation has occurred on its properties; thus neither proof of visual defects nor surface tracking was observed.

## 5 REFERENCES

- [1] D. C. Carmichael and G. T. Noel, "Development of low-cost modular designs for photovoltaic array fields", *IEEE Trans. Power App. Syst.* 104, 5, 1005–1011 (1985).
- [2] J. C. Hernandez, P.G. Vidal, and F. Jurado, "Lightning and Surge Protection in Photovoltaic Installations Power Delivery", *IEEE Transactions* 23, 4, 1961-1971 (2008).
- [3] C. A. Charalambous, N. D. Kokkinos, and N. Christofides, "External Lightning Protection and Grounding in Large-Scale Photovoltaic Applications," *IEEE transactions on electromagnetic compatibility* 56, 22, 427 - 434 (2014).
- [4] H. Häberlin and R. Minkner, "A simple method for lightning protection of PV-systems", *Proc. 12th EPSEC*, Apr. 1994, Amsterdam, Netherlands, pp. 1885–1888.
- [5] H. Häberlin, "Interference voltages induced by magnetic fields of simulated lightning currents in PV modules and arrays", *Proc. 17th EPSEC*, Oct. 2001, Munich, Germany, pp. 2343–2346.
- [6] H. Becker, W. Vaaßen, and F. Vaßen, "Lightning and overvoltage protection in PV and solar thermal systems", *Proc. 16th EPSEC*, May 2000, Glasgow, UK, pp. 2257–2260.
- [7] IEC 61730-2:2004, PV Module Safety Qualification - Part 2: Requirements for Testing.
- [8] V. Perraki and G. Tsolkas, "Temperature dependence on the photovoltaic properties of selected thin-film modules", *International Journal of Renewable and Sustainable Energy* 2, 4, 140-146 (2013).
- [9] T. Michalopoulos and V. Perraki, "Effect of solar radiation incidence angle on the photovoltaic module properties: modelling for Mediterranean sites", *29th EUPVSEC*, Sep. 2014, Amsterdam, Netherlands, pp. 2715-2717.
- [10] IEC 1180-2:1994-06, High-voltage test techniques for low-voltage equipment - Part 2: Test equipment.
- [11] P. Nikolaidis, "Lightning protection of photovoltaic systems", Final year thesis, 2012, University of Patras, Greece.
- [12] Alternative Transients Program (ATP-EMTP), see <http://www.emtp.org/> for double exponential voltage source (last accessed January 2015).